Dissecting Reactor Antineutrino Flux Calculations

A. A. Sonzogni,[1,*] E. A. McCutchan,[1] and A. C. Hayes[2]
[1]National Nuclear Data Center, Building. 817, Brookhaven National Laboratory, Upton, New York 11973-5000, USA
[2]T-2 Theoretical Division MS283, Los Alamos National Laboratory, Los Alamos, New Mexico 8545, USA
(Received 19 April 2017; revised manuscript received 11 July 2017; published 15 September 2017)

Current predictions for the antineutrino yield and spectra from a nuclear reactor rely on the experimental electron spectra from ^{235}U, ^{239}Pu, ^{241}Pu and a numerical method to convert these aggregate electron spectra into their corresponding antineutrino ones. In the present work we investigate quantitatively some of the basic assumptions and approximations used in the conversion method, studying first the compatibility between two recent approaches for calculating electron and antineutrino spectra. We then explore different possibilities for the disagreement between the measured Daya Bay and the Huber-Mueller antineutrino spectra, including the ^{238}U contribution as well as the effective charge and the allowed shape assumption used in the conversion method. We observe that including a shape correction of about $+6\%$ MeV^{-1} in conversion calculations can better describe the Daya Bay spectrum. Because of a lack of experimental data, this correction cannot be ruled out, concluding that in order to confirm the existence of the reactor neutrino anomaly, or even quantify it, precisely measured electron spectra for about 50 relevant fission products are needed. With the advent of new rare ion facilities, the measurement of shape factors for these nuclides, for many of which precise beta intensity data from TAGS experiments already exist, would be highly desirable.

DOI: 10.1103/PhysRevLett.119.112501

The Daya Bay Collaboration has recently published [1] a precise measurement of the inverse beta decay (IBD) cross section folded antineutrino spectrum, revealing that the total number of antineutrinos is 5.4% less than expectations using the ^{235,238}U and ^{239,241}Pu Huber-Mueller [2,3] antineutrino spectra. This deficit is compatible with earlier nuclear reactor antineutrino experiments as analyzed by Mention *et al.* [4], who showed a systematic deficit of antineutrinos at short distances, an effect referred to as the "reactor antineutrino anomaly." Moreover, the shape of the spectrum doesn't agree with the Huber-Mueller model either, as the spectrum is lower than predictions at the peak, and above them for higher energies. This excess of antineutrinos with respect to the Huber-Mueller spectra in the 4.5–7 MeV region is colloquially referred to as the "bump." The other experiments currently measuring θ_{13} near power plants, Double Chooz and RENO, have also reported the anomaly and bump [5,6]. The obvious question is whether this deficit is due to the presence of one (or more) sterile neutrinos, or simply an unknown component in the underlying nuclear physics used in the predictions. New reactor experiments [7–11] aim to answer this question with sophisticated detectors taking measurements at very short baselines.

At the core of the reactor antineutrino anomaly lies how we derive antineutrino spectra for ^{235,238}U and ^{239,241}Pu from the measured electron spectra [12–15]. This procedure is by no means trivial and there has been some effort aimed at addressing the origin of the anomaly and the spectral distortion as well as extensions to the Huber-Mueller approach. Hayes *et al.* [16] postulated potential sources for the bump. Corrections resulting from nuclei produced via neutron capture in the fuel were investigated by Huber and Jaffke [17]. Some efforts have focused on the treatment of first forbidden transitions [18,19]. By jointly analyzing the NEOS and Daya Bay spectra, Huber [20] concluded that ^{239,241}Pu are unlikely sources of the bump. Very recently, by studying the dependence of the IBD antineutrino yield as a function of the Pu amount in the reactors, the Daya Bay Collaboration announced that ^{235}U may be the primary contributor to the reactor antineutrino anomaly [21].

Mougeot [22] has recently published a prescription to calculate spectra following β-minus decay, which has been compared with precisely measured electron spectra. This prescription is somewhat different from that of Huber [2], which was employed to obtain the Huber-Mueller spectra. In this Letter, we look closely at the subtleties used in current predictions to ascertain if basic nuclear physics can provide an explanation to the anomaly. In particular, the compatibility between the Huber and Mougeot prescriptions is explored, and assuming that the ILL-measured electron spectra [12–14] are correct, we use the recently published Daya Bay spectrum to investigate the possibility that the anomaly is due to the ^{238}U contribution, or flaws in the conversion method, such as a deficient knowledge of the Z values needed for the hypothetical branches as well as an allowed shape assumption for them.

The starting point for both conversion and summation methods is the calculation of nuclear level to nuclear level spectra following β-minus decay, which for electrons is given by [2,22]

$$S(E_e) = NW(W^2-1)^{1/2}(W-W_0)^2 \times F(Z_k, W) \times C_L(W) \times C_{\rm fs}(W) \times C_s(Z_k, W) \times C_{\rm wm}(W) \times C_r(Z_k, W) \times C_{\rm exp}(W), \quad (1)$$

where N is a normalization factor so $\int S(E_e)dE_e = 1$; W is the relativistic kinetic energy, $W = E_e/m_ec^2 + 1$, and $W_0 = Q/m_ec^2 + 1$, with Q the total decay energy available also known as the end-point energy; $F(Z_k, W)$ is the Fermi function and Z_k is the number of protons in the daughter nucleus; C_L is the correction factor due to the angular momentum and parity changes in the transition, $C_L = 1$ for allowed decays; $C_{\rm fs}$, C_s, $C_{\rm wm}$, and C_r are the finite size, screening [23], weak magnetism, and radiative correction [24,25] factors; $C_{\rm exp}$ is the correction factor needed to match the experimental data, which is parameterized as

$$C_{\rm exp} = 1 + a_1W + a_2W^2 + a_3W^3 + b_1/W. \quad (2)$$

In the conversion method, the electron spectrum is calculated as

$$S(E_e) = \sum c_m \times S_m(Z_m, Q_m, E_e), \quad (3)$$

where $S_m(Z_m, Q_m, E_e)$ are spectra as given by Eq. (1), Z_m is the effective Z value as a function of the end point energy Q_m, and c_m and Q_m are adjusted to match the experimental data. In the summation method, assuming equilibrium, the spectra per fission are given by [26]

$$S(E) = \sum CFY_i \times S_i(Z_i, E), \quad (4)$$

where CFY_i is the cumulative fission yield and $S_i(E)$ the spectrum from the ith β-minus decaying level in the network, calculated as

$$S_i(Z_i, E) = \sum I_{ik} \times S_{ik}(Z_i, E), \quad (5)$$

with I_{ik} the decay intensity to the kth level in the daughter nucleus, and for electrons, $S_{ik}(E)$ is given by Eq. (1). If the fission yield and decay data are complete, for each of the conversion method branches we should have

$$c_mS(Z_m, Q_m, E) = \sum CFY_iI_{ik}S_{ik}(Z_i, E), \quad (6)$$

where the sum is performed for transitions satisfying $Q_m - \Delta Q_m < Q_{ik} < Q_m + \Delta Q_m$. Assuming a linear Z dependence in the spectra that can be factored out from the energy dependence, and that the latter can be described by the same function for all transitions in the energy interval, that is, $S_m(Z_m, E) \approx (1 + aZ_m) \times S_m(E)$ and $S_m(E) \approx S_{ik}(E)$, we obtain

$$Z_m(Q, \Delta Q) \approx \sum_{ik} Z_k CFY_i I_k / \sum_{ik} CFY_i I_k. \quad (7)$$

The current standard conversion calculations are those by Huber [2], who used Fermi functions and finite size corrections as given by Wilkinson [27], as well as a weak magnetism term $C_{\rm wm}(W) = (1 + 0.67 \times 10^{-2} \times 0.511 \times W)$, obtained by fitting a low-Z, low-log ft nuclear data sample. Mougeot [22] recently reviewed the world data of precisely measured beta spectra, deducing shape factors $C_{\rm exp}$ for about 110 β-minus transitions; however, Mougeot didn't use weak magnetism corrections and obtained Fermi functions with finite size corrections by solving the corresponding electron Dirac equations [23], which produces nearly identical values to those tabulated by Behrens and Jänecke [28]. It turns out that both the Huber and Mougeot prescriptions produce very similar results due to the compensating effects of the different Fermi functions, finite size, and weak magnetism corrections used.

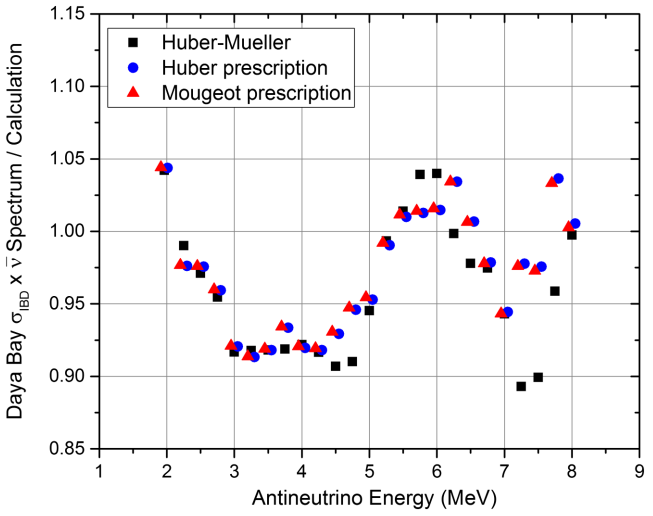

FIG. 1. Daya Bay measured IBD cross section folded antineutrino spectrum divided by the calculated ones using the Huber and Mueller antineutrino spectra (black squares), as calculated in this work using the Huber prescription (blue circles), and as calculated using the Mougeot prescription (red triangles). To facilitate the viewing, uncertainties were not plotted and the Huber (Mougeot) prescription points are shifted to higher (lower) energies by 0.05 MeV.

To illustrate the level of numerical similarity between both prescriptions, Fig. 1 shows the measured Daya Bay spectrum divided by calculations using the published Huber-Mueller antineutrino spectra and our calculations using the Huber or Mougeot prescriptions. In our calculations (a) reactor start up or shut down and fuel storage effects were not applied, (b) the $Z_m(Q, \Delta Q)$ functions are from Eq. (7) using the JEFF-3.1 fission yields [29] and updated ENDF/B-VII.1 decay data [30], (c) some Q_m values were fixed to those of main contributors such as ^{96}Y and ^{92}Rb, (d) conversion calculations were also performed on summation electron spectra to check for biases [31], (e) for ^{238}U we used the summation method with the same set of fission yields and decay data, (f) IBD cross sections are from Ref. [32], (g) $C_{\rm exp}$ was taken as 1. The small difference of less than 1% in terms of anomaly effect, between the Huber-Mueller values and our

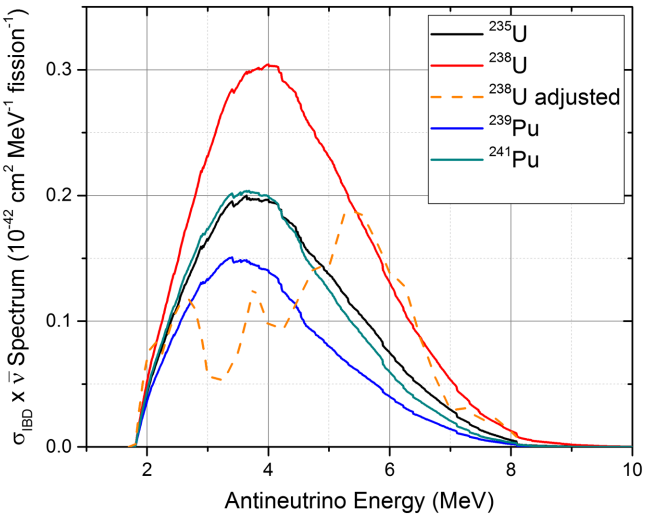

FIG. 2. Antineutrino spectra calculated using the summation method multiplied by the IBD cross section for ^{235,238}U and ^{239,241}Pu (full lines). The dashed line corresponds to the ^{238}U antineutrino spectrum adjusted to match the measured Daya Bay antineutrino spectrum.

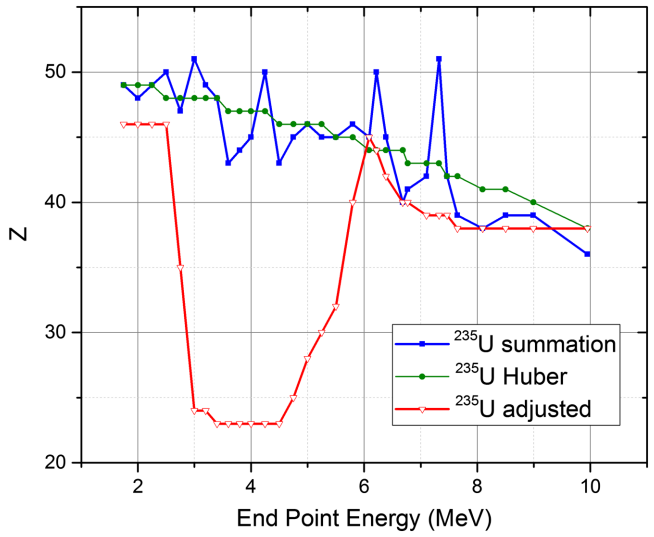

FIG. 3. Effective Z values as a function of the end-point energy used in the conversion method for ^{235}U.

calculation using the Huber prescription is probably due to the use of different Z_m and Q_m values, as well as the polynomial fit to the spectra. We note also that the high-energy half of the "bump" is dependent on the Q_m values, becoming far less distinct with our particular choice.

Having established the numerical similarity between both Huber and Mougeot prescriptions, very important as the latter has been validated against the body of available experimental data, we proceed to explore several scenarios that could explain the anomaly originating from deficiencies in the underlying data or methods. We start with the ^{238}U contribution, since its electron spectrum is the least known, to the point that the conversion method is not applicable and one must rely on the summation method [3,26]. It has been speculated [16] that the bump may reflect our deficient knowledge of the ^{238}U antineutrino spectrum, since ^{238}U produces more energetic antineutrinos than ^{235}U and ^{239,241}Pu. One way, albeit somewhat naive but illustrative nevertheless, of testing if the discrepancy between the Daya Bay spectrum and the Huber-Mueller predictions is due to the lack of an accurate ^{238}U spectrum is to adjust it to match the Daya Bay measurement. If the resulting adjusted spectrum is physically feasible, this would point to the need for a new ^{238}U electron spectrum measurement. Results are shown in Fig. 2 for the original and adjusted ^{238}U IBD cross section folded antineutrino spectra. For comparison, the ^{235}U and ^{239,241}Pu antineutrino spectra obtained from the summation method are also plotted. Clearly, the ^{238}U adjusted result is unrealistic as (a) the shape is dramatically different from that of the other actinides, (b) despite being more neutron rich than ^{235}U, its IBD antineutrino yield would be similar, that is, would not follow a $(3Z - A)$ systematics [33], and (c) the electron spectrum as measured by Haag *et al.* [15] exhibits no anomalous features.

We explore now the possibility of the effective Z as a source of the discrepancy as the Fermi function Z dependence shifts the electron to lower (higher) energies for higher (lower) Z values. It is conceivable then to speculate that due to deficiencies in the fission yield and/or decay data, our knowledge of $Z_m(Q, \Delta Q)$ is incomplete. As done for ^{238}U, we explore this idea by adjusting $Z_m(Q, \Delta Q)$ in the conversion method to match the Daya Bay spectrum. Results for ^{235}U are shown in Fig. 3, compared with Huber's and the present summation results using Eq. (7). Similar results were obtained for ^{239,241}Pu, which are not shown in the plot for clarity's sake. In order to match the Daya Bay data, a $Z_m(Q)$ value near 25 is needed for end point energies of around 4 MeV, which definitely allows us to rule out this scenario as this value is below even the smallest Z significantly populated in binary fission.

In previous conversion calculations, all the average branches had the shape factors, C_{exp}, set equal to one. This is due to the lack of complete experimental data, but also supported by the assumption that with a large number of β-minus decaying levels in the network, individual shape effects would cancel out. Earlier publications [33–35] have shown that the number of nuclides contributing to the antineutrino spectra bump is not very large. We revisit this point in Fig. 4, where the total number of β-minus decaying levels in the network, obtained from a summation calculation, is plotted as a function of the antineutrino energy for the Daya Bay reactors, highlighting the number of levels needed to account for 25%, 50%, 90%, and 99% of the spectrum. For energies higher than 3 MeV, 75% of the spectrum can be accounted by 50 or fewer levels out of the total 700. It is then possible that the average spectra

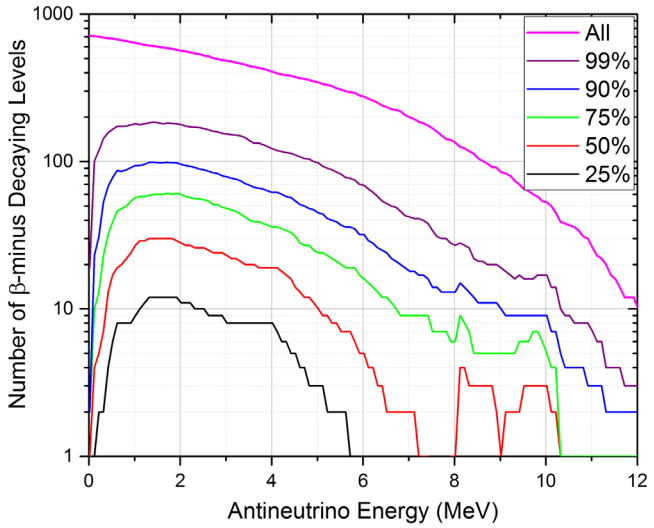

FIG. 4. Number of β-minus decaying levels as a function of the antineutrino energy for the Daya Bay reactors, together with the number of levels needed to account for 25%, 50%, 90%, and 99% of the antineutrino spectrum.

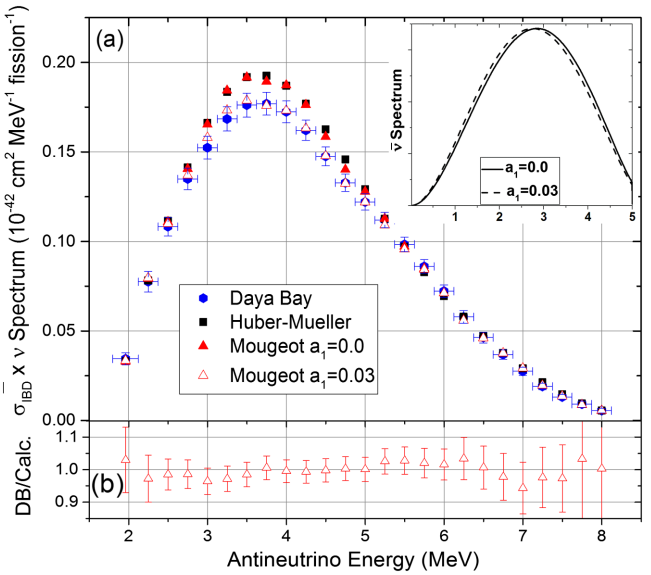

FIG. 5. (a) Daya Bay spectrum and predictions using the Huber-Mueller spectra and our Mougeot-prescription spectra with and without a linear term (a_1) equal to 0.03 for transitions with end-point energy in the 3–6 MeV region. The antineutrino spectra for these a_1 values for $Z = 45$ and $Q = 5$ MeV are shown in the inset. (b) Ratio of Daya Bay spectrum to Mougeot prescription calculations with $a_1 = 0.03$. For clarity, calculation uncertainties are not plotted.

used in the conversion method would retain some shape corrections different from unity. Shape corrections are expected for many of the nuclides undergoing β-minus decay in a reactor, either from first-forbidden transitions that may require them [18,19], or from allowed transitions which could have shape corrections arising from second-order contributions such as weak magnetism as they are of Gamow-Teller type. Inspired by this, we explored the sensitivity of the Daya Bay data to C_{exp}, by adjusting the a_1 parameter of Eq. (2) in a conversion method calculation for ^{235}U and ^{239,241}Pu to match the Daya Bay spectrum. We find that an a_1 value of $+0.03$ for transitions with end-point energies in the 3–6 MeV region will improve the agreement with the Daya Bay data considerably, as shown in Fig. 5. This positive linear term boosts the electron spectra, and in turn, shifts the antineutrino spectra to lower energies, illustrated in the inset of Fig. 5, as it would a reduction in Z_{eff}. This a_1 value corresponds to a slope in the ratio of the corrected electron spectrum to uncorrected one of $+6\%$ MeV^{-1}.

While there have been high-quality measurements of shape factors for light nuclides, most notably for ^{12}B obtaining an a_1 value of $+0.48\%$ MeV^{-1} [36], only Q values and strength functions derived from the electron spectra from nuclides relevant to the reactor anomaly, that is, end point energies larger than 3 MeV, have been reported [37,38]. Therefore, there is no experimental evidence that will allow us to rule out an a_1 value of 0.03. The work of Mougeot, however, reveals some intriguing results, for instance, in the allowed decay of ^{130,131}I, a_1 values, values of $+0.04$ and $+0.02$ were obtained. Another interesting result is that Huber [2] obtained a weak magnetism term, albeit highly uncertain, equal to $+4.78\%$ MeV^{-1} for all nuclides in the sample. Finally, and simply to illustrate how relevant C_{exp} is to the conversion method, the reactor anomaly would increase to about 12% if all the branches would have a C_{exp} equal to that of ^{144}Pr as given by Mougeot [22]. ^{144}Pr will be used in the SOX experiment [39] and most likely its electron spectrum will be measured with high precision. Similarly, for a nuclear reactor, we must precisely determine C_{exp} values for the most relevant nuclides to fully understand the interrelation among the total electron and antineutrino spectra.

In summary, we first compared the Mougeot and Huber prescriptions to calculate level to level electron and antineutrino spectra and found them numerically similar due to compensating effects between the Fermi functions, finite size and weak magnetism corrections. Then, in order to understand the disagreement between the Daya Bay's measured antineutrino spectrum with the Huber-Mueller predictions, we explored the feasibility of the ^{238}U spectrum and the effective Z as possible sources by adjusting them to match the measured Daya Bay spectrum. Both scenarios are ruled out, as the adjusted ^{238}U antineutrino spectrum has an unphysical shape, smaller integral than expected from systematic trends, and is inconsistent with measurement; while the fitted Z effective would correspond to fission products with negligible fission yield. Finally, we explored the sensitivity to experimental shape factor corrections and found that using a linear term equal to $+0.03$ in the conversion method results in a much closer agreement

with the Daya Bay spectrum. Unlike the two previous cases, this scenario cannot be ruled out because of an absence of precisely measured electron spectra from the relevant fission products. Previously, it was noted the importance of β intensities [40,41] and fission yields [42] for the summation method. This sensitivity analysis demonstrates the significance of experimental shape factors for both conversion and summation calculations. One possible way forward to confirm or refute the existence of the anomaly would be to precisely measure the shape for the relevant nuclides, incorporate them in summation calculations to understand their effect, and finally, through an average procedure, include them in conversion calculations.

As was shown, for energies above 3 MeV, 75% of the spectrum is accounted for by fewer than 50 β-minus decaying levels, dispelling the idea that studying the decay characteristics of nuclides contributing to reactor's anti-neutrino spectra is impractical due to an impossibly large number of individual contributors. The shape measurement would also yield mean gamma and beta energies [43] needed for decay heat calculations, complementing and confirming the TAGS results already available for many of these nuclides [35,41,44,45]. As an analogy, the number of nuclides contributing ~98% of a reactor β-delayed neutron yield is ~40 and measurements of their half-lives, neutron emission probabilities, and neutron spectra were performed over 30 years ago [46].

Work at Brookhaven National Laboratory was sponsored by the Office of Nuclear Physics, Office of Science of the U.S. Department of Energy under Contract No. DE-AC02-98CH10886. Work at Los Alamos National Laboratory was funded by the Los Alamos National Laboratory LDRD program. We are grateful to X. Mougeot for making available his code to calculate electron and antineutrino spectra.

*sonzogni@bnl.gov

[1] F. P. An *et al.*, Phys. Rev. Lett. **116**, 061801 (2016).
[2] P. Huber, Phys. Rev. C **84**, 024617 (2011).
[3] T. A. Mueller *et al.*, Phys. Rev. C **83**, 054615 (2011).
[4] G. Mention, M. Fechner, Th. Lasserre, Th. A. Mueller, D. Lhuillier, M. Cribier, and A. Letourneau, Phys. Rev. D **83**, 073006 (2011).
[5] Y. Abe *et al.*, Phys. Rev. Lett. **108**, 131801 (2012). For latest results see A. Cabrera Serra, CERN seminar Sept. 20, 2016, available at https://indico.cern.ch/event/548805/.
[6] J. H. Choi *et al.*, Phys. Rev. Lett. **116**, 211801 (2016).
[7] J. Ashenfelter *et al.*, Nucl. Instrum. Methods Phys. Res., Sect. A **806**, 401 (2016).
[8] G. Boireau *et al.*, Phys. Rev. D **93**, 112006 (2016).
[9] Y. Ko *et al.*, J. Korean Phys. Soc. **69**, 1651 (2016).
[10] N. Ryder (SoLid Collaboration), *Proc. Sci.*, EPS-HEP2015 (2015) 071.
[11] V. Helain (Stereo Collaboration), arXiv:1610.00003.
[12] F. von Feilitzsch, A. A. Hahn, and K. Schreckenbach, Phys. Lett. B **118**, 162 (1982).
[13] K. Schreckenbach, G. Colvin, W. Gelletly, and F. Von Feilitzsch, Phys. Lett. **160B**, 325 (1985).
[14] A. A. Hahn, K. Schreckenbach, W. Gelletly, F. von Feilitzsch, G. Colvin, and B. Krusche, Phys. Lett. B **218**, 365 (1989).
[15] N. Haag, A. Gütlein, M. Hofmann, L. Oberauer, W. Potzel, K. Schreckenbach, and F. M. Wagner, Phys. Rev. Lett. **112**, 122501 (2014).
[16] A. C. Hayes, J. L. Friar, G. T. Garvey, D. Ibeling, G. Jungman, T. Kawano, and R. W. Mills, Phys. Rev. D **92**, 033015 (2015).
[17] P. Huber and P. Jaffke, Phys. Rev. Lett. **116**, 122503 (2016).
[18] A. C. Hayes, J. L. Friar, G. T. Garvey, G. Jungman, and G. Jonkmans, Phys. Rev. Lett. **112**, 202501 (2014).
[19] D.-L. Fang and B. A. Brown, Phys. Rev. C **91**, 025503 (2015).
[20] P. Huber, Phys. Rev. Lett. **118**, 042502 (2017).
[21] F. P. An *et al.*, Phys. Rev. Lett. **118**, 251801 (2017).
[22] X. Mougeot, Phys. Rev. C **91**, 055504 (2015).
[23] H. Behrens and W. Bühring, *Electron Radial Wave Function and Nuclear Beta Decay* (Clarendon, Oxford, 1982).
[24] A. Sirlin, Phys. Rev. **164**, 1767 (1967).
[25] A. Sirlin, Phys. Rev. D **84**, 014021 (2011).
[26] P. Vogel, G. K. Schenter, F. M. Mann, and R. E. Schenter, Phys. Rev. C **24**, 1543 (1981).
[27] D. H. Wilkinson, Nucl. Instrum. Methods Phys. Res., Sect. A **290**, 509 (1990).
[28] H. Behrens and J. Jänecke, in *Numerical Tables for Beta-decay and Electron Capture*, edited by H. Schopper, Landolt-Börnstein Vol. 4 (Springer-Verlag, Berlin, 1969).
[29] M. A. Kellett, O. Bersillon, and R. W. Mills, JEFF REPORT 20, OECD, ISBN 978-92-64-99087-6 (2009).
[30] M. B. Chadwick *et al.*, Nucl. Data Sheets **112**, 2887 (2011).
[31] P. Vogel, Phys. Rev. C **76**, 025504 (2007).
[32] A. Strumia and F. Vissani, Phys. Lett. B **564**, 42 (2003).
[33] A. A. Sonzogni, T. D. Johnson, and E. A. McCutchan, Phys. Rev. C **91**, 011301(R) (2015).
[34] D. A. Dwyer and T. J. Langford, Phys. Rev. Lett. **114**, 012502 (2015).
[35] A.-A. Zakari-Issoufou *et al.*, Phys. Rev. Lett. **115**, 102503 (2015).
[36] C. S. Wu, Y. K. Lee, and L. W. Mo, Phys. Rev. Lett. **105**, 202501 (2010).
[37] R. Decker, K. D. Wunsch, H. Wollnik, E. Koglin, G. Siegert, and G. Jung, Z. Phys. A **294**, 35 (1980).
[38] R. Iafigliola, Ph.D. Thesis, McGill University, 1985.
[39] G. Bellini *et al.* (SOX Collaboration), J. High Energy Phys. 08 (2013) 038.
[40] M. Fallot *et al.*, Phys. Rev. Lett. **109**, 202504 (2012).
[41] B. C. Rasco *et al.*, Phys. Rev. Lett. **117**, 092501 (2016).
[42] A. A. Sonzogni, E. A. McCutchan, T. D. Johnson, and P. Dimitriou, Phys. Rev. Lett. **116**, 132502 (2016).
[43] G. Rudstam, P. I. Johansson, O. Tengblad, P. Aagaard, and J. Eriksen, At. Data Nucl. Data Tables **45**, 239 (1990).
[44] R. C. Greenwood, R. G. Helmer, M. H. Putnam, and K. D. Watts, Nucl. Instrum. Methods Phys. Res., Sect. A **390**, 95 (1997).
[45] A. Algora *et al.*, Phys. Rev. Lett. **105**, 202501 (2010).
[46] M. C. Brady, Los Alamos National Laboratory Report No. LA-11534-T (1989).